Hydrocarbons Adsorbed to Combustion-Derived PM Localize to Lipid Droplets and Activate Oxidative Stress Response Genes In Respiratory Cells (128910)

Arthur L. Penn, Gleeson Murphy*[1], Rodney L. Rouse*[2] and William W. Polk**

**Comparative Biomedical Sciences, School of Veterinary Medicine, Louisiana State University, Skip Bertman Drive, Baton Rouge, LA 70803. [1] Present address: U.S. Army Veterinary Medical Corps, Analytical Toxicology Division, USAMRICD, Aberdeen, MD, 21010-5400. [2] Present address: U.S. Food and Drug Administration, CDER, OPS, OTR, Department of Applied Pharmacology Research, White Oak Campus, Silver Spring, MD 20993.*

Airborne particles, especially those arising from combustion and industrial processes, are of increasing environmental and public health concern due to a) their contribution to ambient pollution and b) the toxic responses they elicit, especially in people already at risk for cardiovascular and respiratory diseases. The varied toxic responses have been attributed both to physical and chemical characteristics of the particles (**1,2**).

Among physical characteristics, particle size is inversely associated with particle toxicity, at least in part, because the smaller the particle, the more likely it is to penetrate deeply into the lungs. In addition, smaller particles provide greater available surface area for adsorption of toxic agents than do larger particles of equivalent mass.

There is growing evidence of deleterious health effects associated with inhalation of particulate matter (PM) in the fine (<2.5 μ) and ultrafine (<0.1 μ) size ranges (**3**). Cigarette smoke and diesel exhaust (DEP) are among the most common, and intensively studied, sources of complex particulates. Organic chemicals adsorbed to DEP elicit pro-inflammatory and oxidative stress responses in respiratory system cells following DEP exposure both *in vivo* and *in vitro* (**4-9).** Cigarette smoke, whose contributions to major diseases, including lung cancer and cardiovascular disease, have been documented exhaustively for over a half century, contains > 4,500 chemical components, of which at least 100, including benzo(a)pyrene [B(a)P] and other carcinogens, are polynuclear aromatic hydrocarbons (PAHs; **10**). Organic chemical-rich products of incomplete combustion (soots) also are released to the atmosphere in large quantities in petrochemical-related processes, e.g., during routine flaring of volatiles. In addition, sabotage and accidents involving pipelines and refineries, pose major risks both in the U.S. and abroad.

We have been investigating the *in vivo* and *in vitro* responses to exposure to butadiene soot (BDS), which serves as both a model mixture and real-life example of PAH-rich, combustion-derived nanoparticles (**11-14**). 1,3-butadiene, an aliphatic hydrocarbon by-product of petroleum refining, is a "top 40" U. S. chemical and is the starting material for virtually all commercially produced rubber. Early, during combustion of petrochemical volatiles, hydrocarbon free radicals are formed. These can fuse, ultimately giving rise to PAHs, which can aggregate into nanoparticles and then into extended, branched-chain soots (**15**). Generation as well as physical and chemical characterization of the branched-chain BDS, composed of 20-50 nm, PAH-rich, carbonaceous particles, has been described (**11**). The characteristic blue fluorescence of PAHs allows the time-and dose-dependent uptake of BDS by cells to be followed and recorded (**11-13).**

Human broncho-epithelial cells exposed to BDS develop blue fluorescence, which over time becomes localized in discrete cytoplasmic vesicles (**11**). Following BDS exposure, these cells display the same profile of extractable PAHs as the parent BDS. The fluorescence does not develop if the cells are exposed to carbon black instead of BDS, or if the BDS is extracted with organic solvents before the soot particles are presented to the cells.

The experiments described here were designed to identify the cytoplasmic compartment(s) within which BDS-associated fluorescence is localized and to determine whether there is concomitant activation of xenobiotic metabolism pathways known to potentiate PAH toxicity. Complete details of these studies have recently been published (**13**).

Methods

Cell Culture. Cells (1.5 x 10^6) of the BEAS-2B human broncho-epithelial cell line (**16**), were grown in bronchial-epithelial growth medium (BEGM; Cambrex, Walkersville, MD), before expansion in T-150 flasks.

Cells (1 x 10^6) of the MH-S mouse alveolar macrophage cell line (**17**), were grown in RPMI 1640 medium with 10% FBS to 80–90% confluence.

Mouse 3T3-L1 preadipocytes (**18**) were grown to 2 days post-confluence in DMEM with 10% CS and induced to differentiate in DMEM supplemented with 4.5 g/L glucose, 10% FBS, 100 U/mL penicillin, 100 µg/mL streptomycin, 0.5 mM 3-isobutyl-methylxanthine, 1 µM dexamethasone, and 1.7 µM insulin. After 48 hrs, this medium was replaced with DMEM containing 4.5 g/L glucose supplemented with 10% FBS (**19**).

BDS Generation and Collection. The process of BDS generation and collection has been described in detail (**11**).

BDS Exposures. In all cases, the medium was changed immediately before addition of BDS or staining solutions. BDS stock solution was prepared by sonicating 10 mg BDS in 50 mL of medium (3 15-second pulses of a Model 450 Branson Sonifier, Danbury, CT). BEAS-2B cells, MH-S cells, and adipocytes were exposed to 20 µg/mL sonicated BDS for 24 hours prior to fluorescence imaging. For microarray and/or quantitative real time (qRT)-PCR experiments, BEAS-2B and MH-S cells were exposed to BDS for 0, 1, 3, or 24 hours prior to RNA extraction.

Fluorescent Dye Co-Localization. Organelle-specific fluorescent probes (Molecular Probes, Invitrogen; Carlsbad, CA) for lysosomes, autophagosomes, endosomes, mitochondria, endoplasmic reticulum and lipid droplets were used to investigate candidate organelles for the localization of BDS-associated fluorescence. To investigate peroxisomes as candidate organelles we transfected BEAS-2B cells with a plasmid whose protein product is a fusion of the red fluorescent protein DsRed2 with the peroxisomal targeting sequence 1 [PTS1] (**20**).

Fluorescence Microscopy. We used a Zeiss Axiovert 405M inverted fluorescence microscope (40X) with a Microfire Megapixel Digital CCD camera, operated by PictureFrame software (Optronics; Goleta, CA) and a Leica DM RXA2 upright microscope, equipped with differential interference contrast (DIC) optics (40X, 63X, 100X)--with a SensiCam QE 12-bit, cooled CCD camera (Cooke; Romulus, MI), operated by SlideBook software (Intelligent Imaging Innovations; Denver, CO). We used SlideBook to measure lipid droplet dimensions and Adobe Photoshop CS to process all images.

Cytotoxicity Assay. We assessed cell viability with the Cell Counting Kit-8 (Dojindo Molecular Technologies (Gaithersburg, MD). Cells were exposed to sonicated BDS for 1, 4, 8, or 24 hours. Unexposed sets of control cells were used for comparison at each time point.

RNA Isolation. BEAS-2B cells and MH-S cells at or near confluence were scraped into 1 mL of Invitrogen TRIzol Reagent and passed 3X through a 23G needle. RNA was isolated by TRIzol/chloroform extraction, followed by column purification (Qiagen RNeasy Mini Kit). RNA quality and integrity was assessed using the Agilent RNA 6000 Nano Assay Kit and the Agilent 2100 BioAnalyzer (Santa Clara, CA). Total RNA was converted to cDNA using TaqMan Reverse Transcriptase Reagents (Applied Biosystems; Foster City, CA).

pDsRed-Monomer-C-ADFP Plasmid Preparation and Transformation. Human ADFP PCR primers were as designed (**21**) from the ADFP mRNA sequence in GenBank: a) 5'-GGGGCAGGTTTAATGAGTTTTATG-3'; and b) 5'-CCAGGAAGAAAAAT GGCATCCGTT-3' (Integrated DNA Technologies; Coralville, IA). PCR (30 cycles) was performed on 50 ng of BEAS-2B cDNA in a PTC-100 thermal cycler (MJ Research, Waltham, MA). To impart red fluorescence to ADFP expressed within cells, the ADFP PCR product was ligated into the pDsRed-Monomer-C In-Fusion Ready Vector (Clontech; Mountain View, CA) as described (**13**). BEAS-2B cells grown on glass coverslips in 60 mm dishes were transformed with 500 ng of the plasmid, in the presence of Lipofectamine LTX and PLUS reagents (Invitrogen). After 48 hours, cells were observed for lipid droplet fluorescence and then exposed to BDS (20 µg/mL) for 24 hours prior to imaging for co-localization.

Gene Microarray Assay. Global gene expression in BEAS-2B cells was assessed from total RNA on Affymetrix Human Genome U133 Plus 2.0 Arrays that were processed at the Research Core Facility of the LSU Health Science Center-Shreveport. All gene chips and instrumentation were from Affymetrix (Santa Clara, CA). All data collected and analyzed here adhere to the guidelines for Minimal Information About a Microarray Experiment (MIAME).

Quantitative Real Time (qRT)-PCR. qRT-PCR was performed on cDNA samples from BEAS-2B and MH-S cells with inventoried TaqMan Gene Expression Assays primer-probe sets (Applied Biosystems) for selected genes. Relative gene expression was determined by the comparative cycle threshold ($\Delta\Delta C_T$) method, with each gene normalized to β-actin (ACTB) for human cells (***22***) or hypoxanthine guanine phosphoribosyl transferase (Hprt1) for mouse cells (***23***), and then compared to the 0 hour control. Results are reported as fold change over control. Standard error of the mean [$(2^{-\Delta\Delta CT}) \pm$ SEM] was used to determine significant at $\alpha = 0.05$.

Statistical Analysis. We used the GLM procedure of the SAS statistical package (version 9.1.3; SAS Institute, Inc., Cary, NC) to compare RT-PCR data, and Dunnett's *t* test to determine statistical differences. Gene chip data, filtered to remove data from non-functional probe sets, were analyzed at each time point by pair-wise comparisons of gene expression in BDS-treated vs. control cells (Expression Analysis, Durham, NC). Gene expression was expressed as log ratio for these comparisons. All transcripts reported here had a fold change (up or down) of at least 1.5X and both an individual p-value and a false discovery rate < 0.05. Gene expression data were analyzed with the network- and pathway-building software, Ingenuity Pathways Analysis 4.0; gene networks and canonical pathways were examined using the Ingenuity Analysis Knowledge Database (Ingenuity Systems, Redwood City, CA).

Results

BDS-Associated Fluorescence in Human Broncho-Epithelial Cells is Time-Dependent

Within 30 minutes after BEAS-2B cells are exposed to BDS, a diffuse blue fluorescence appears in each of the cells (Figure 1a). By 2-4 hours, the diffuse fluorescence is replaced by bright, punctate fluorescence that is visible clearly within cytoplasmic vesicles (Figure 2b). The fluorescence intensifies over the next 20 hours and then plateaus for an additional 48 hours, in the absence further addition of BDS (figure 1c). No nuclear fluorescence is evident.

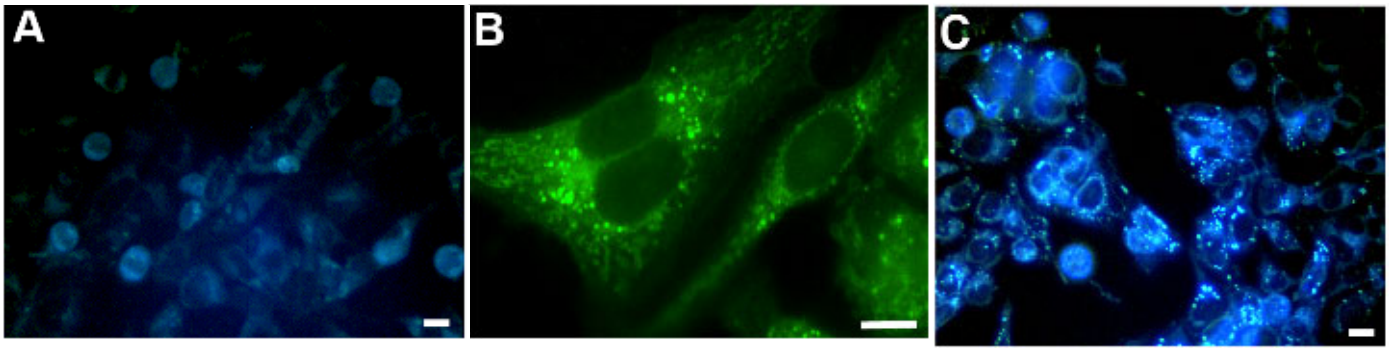

Figure 1: Time-dependent fluorescent responses of BEAS-2B cells exposed to petrochemical combustion-derived ultrafine particles (BDS) sprinkled on the surface of the culture medium. Diffuse fluorescence is visible within 10-30 min (A). There is a transition from diffuse to punctate fluorescence by 2 hours post-exposure (B). Punctate fluorescence increases in intensity through the first 4 hours of exposure to BDS (C). Ultraviolet excitation wavelengths (~360 nm) typically provided the brightest emission spectra for visualization of the BDS-associated fluorescence as shown in A and C; however, the extensive punctate fluorescence shown in B was best demonstrated with a longer excitation wavelength (~480 nm). Bars = 10 μm.

Alveolar Macrophages and Adipocytes also Display BDS-Associated Fluorescence

Mouse alveolar macrophages (Figure 2b) exhibit fluorescence in larger peri-nuclear vacuoles (1.8± 0.2μ) than are present in human bronco-epithelial cells (figure 2a). Fluorescent vacuoles in cultured

mouse adipocytes are even larger (2.6±0.3μ) than those appearing in the macrophages (Figure 2c). Development of punctate BDS-associated fluorescence in all three cell types is time-dependent (data not presented).

BDS Exposure Does Not Alter Cell Viability Through 24 Hours of Exposure

Peripheral membrane blebs, often indicative of cell damage, appeared in some BEAS-2B cells after 24 hours of exposure. Therefore, we assessed cell viability of both BEAS-2B and MH-S cells. A formazan-based dye assay indicated that viability was unaffected in each of these cell lines for up to 24 hours after exposure to BDS (data not presented).

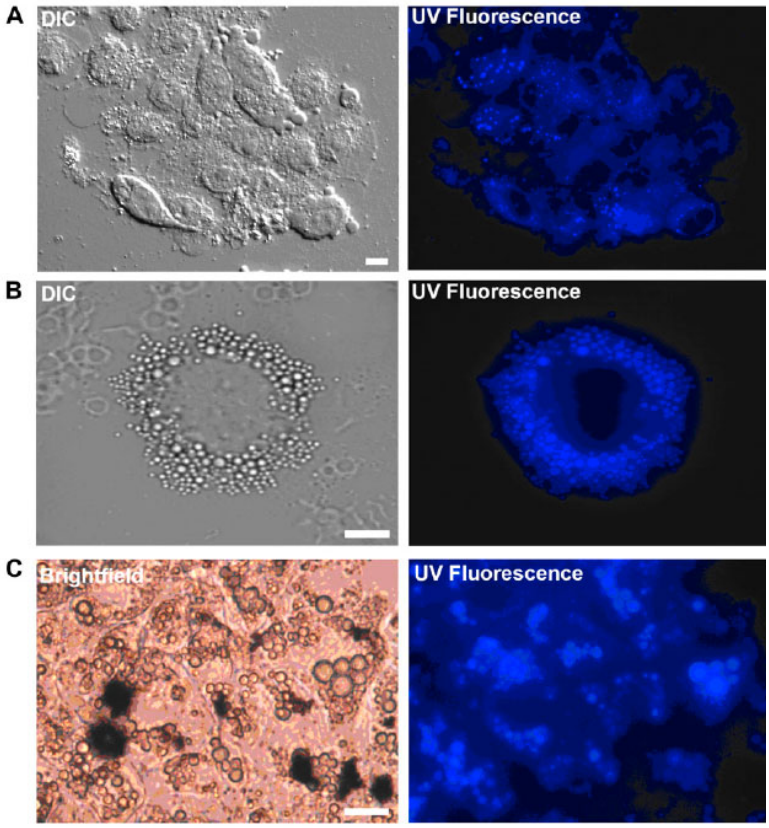

Figure 2. Broncho-epithelial cells, alveolar macrophages and adipocytes display characteristic BDS-associated fluorescence. Differential interference contrast (DIC) (A, B) and bright-field photomicrographs (C) paired with ultraviolet-fluorescence images of BEAS-2B human broncho-epithelial cells (A), MH-S murine alveolar macrophages (B), and 3T3-L1 murine adipocytes (C) after a 24-hour exposure to sonicated BDS. The fluorescent bodies appear as variably sized refractile bodies; peripheral membrane blebs are visible on some cells (A). In contrast to BEAS-2B cells, MH-S cells displayed larger droplets, all of which were fluorescent (B). Large droplets in mouse adipocytes displayed BDS-associated fluorescence (C). Black BDS particles are visible in the bright-field panel of C, and the fluorescent panel demonstrates the lack of fluorescence associated with the particles. Bars 5 10 mm (A), 7.5 mm (B), and 10 mm (C).

BDS-Associated Fluorescence is Localized Within Cytoplasmic Lipid Droplets in Target Cells

Based on light microscope observations of size and cytoplasmic localization, candidate organelles were selected and tested by fluorescence co-localization, to identify those in which the punctate fluorescence was concentrated. The candidate organelles included lysosomes, autophagosomes, endosomes, peroxisomes, mitochondria, endoplasmic reticulum and lipid droplets. Fluorescent markers specific for each organelle were tested for co-localizatjon with the blue BDS-associated fluorescence. The emission maxima of all the markers were in the red region, insuring that the red and blue fluorescence responses would be readily distinguishable from each other, unless they overlapped, in which case the resulting color would be purple.

The BDS-associated blue fluorescence co-localized only with the red cholesterol-BODIPY C_{11} marker, yielding a purple fluorescence (data not presented). Cholesterol-BODIPY C_{11} concentrates within hydrophobic compartments of cells, via the "selective" transport pathway. This pathway directs lipoprotein-derived cholesteryl esters to lipid droplets without their first having to pass through either

the Golgi apparatus or lysosomes. Lipid droplet localization of the BDS-associated fluorescence was confirmed by transfecting BEAS-2B cells with a plasmid whose protein product is a fusion of a red dye monomer with a lipid droplet membrane-specific protein, ADRP. The plasmid-transfected cells displayed a large number of fluorescent red cytoplasmic inclusions. One such cell at 100x is shown in Figure 3a. The BDS-associated blue cytoplasmic inclusions in the same cell are shown in Figure 3b. When the two images are merged (Figure 3c) there is complete co-localization of the red and blue fluorescent images, resulting in the purple inclusions (i.e., lipid droplets) seen in Figure 3c.

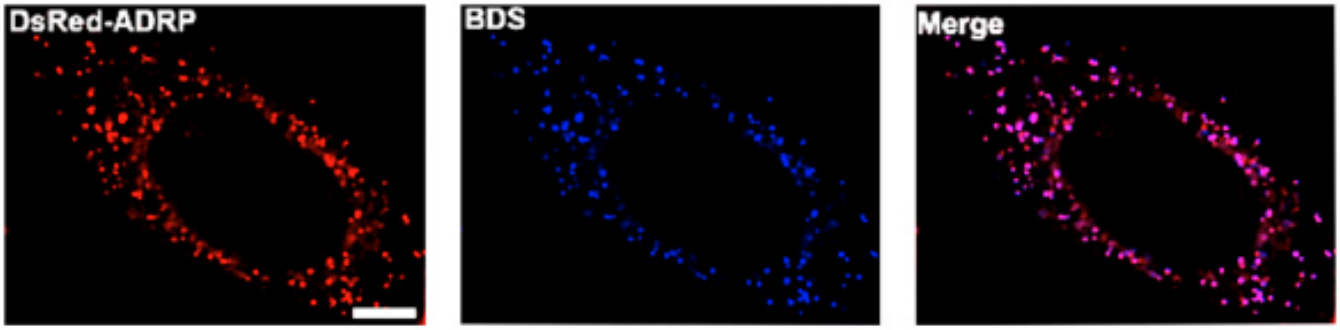

Figure 3: Co-localization of a lipid droplet-specific probe with BDS fluorescence in BEAS-2B cells. Left panel; red fluorescence resulting from lipid droplet localization of the DsRed-ADRP tag; center panel: subcellular localization of the BDS-associated blue fluorescence; right panel: complete co-localization of the red and blue fluorescent images, yielding the purple image shown.

BDS Stimulates Time-Dependent Expression of Aryl Hydrocarbon Receptor (AHR)-Induced and Oxidative Stress Response Genes in BEAS-2B Cells

There were time-dependent changes in gene expression, assessed by analysis of microarray data, in BEAS-2B cells exposed to BDS for 1-24 hr. Of the 448 differentially-regulated genes identified at 24 hours, 70 were down-regulated and 378 were up-regulated. Up-regulated genes (Table 1) included AHR-responsive genes (e.g., AHR repressor, cytochrome P450 1A1 and 1B1) and nuclear erythroid-2 factor 2(NRF2)-mediated oxidative stress response genes (e.g., FOS, NQO1). These results were confirmed in BEAS-2B cells and demonstrated in MH-S cells by qRT-PCR.

TABLE 1. TIME-DEPENDENT MICROARRAY CHANGES IN ARYL HYDROCARBON RECEPTOR– AND NRF2-RELATED GENE EXPRESSION IN BUTADIENE SOOT–EXPOSED BEAS-2B CELLS*

	BEAS-2B Microarray		
	1 h	3 h	24 h
AhR-induced response			
AHRR	1.1	1.9	1.6
ALDH1A3	1.1	2.4	3.2
CYP1A1	2.3	14.7	29.7
CYP1B1	3.3	5.4	4.1
IL1A	3.4	2.5	5.1
IL1B	2.6	2.9	5.3
TIPARP	6.3	5.0	5.7
NRF2-mediated oxidative stress			
FOS	2.1	1.2	2.0
NQO1	1.1	1.2	2.0
TXN	−1.2	1.1	2.1
MAFF	3.6	4.2	5.1
JUN	1.4	1.4	2.3
DNAJB6	−1.1	1.3	2.1

* Results for each gene at each time point are reported as fold change in a single pairwise comparison relative to control sample.

TABLE 2. TIME-DEPENDENT QUANTITATIVE REAL-TIME–PCR EXPRESSION CHANGES IN ARYL HYDROCARBON RECEPTOR–RELATED GENES OF BEAS-2B AND MH-S CELLS EXPOSED TO BUTADIENE SOOT FOR 24 h*

	BEAS-2B		MH-S	
	1 h	24 h	1 h	24 h
AhR-induced response				
AHRR†	n/a	n/a	3.6‡	3.3‡
ALDH1A3	1.5	4.4‡	1.4	1.4
CYP1A1	21.5	108.4‡	10.5‡	6.4‡
CYP1B1	6.1‡	3.5	69.2‡	17.6‡
IL1A	6.8‡	4.9‡	n/a	n/a
IL1B	6.1‡	5.1‡	1.0	1.0
TIPARP	13.1‡	3.5	7.8‡	2.0‡

Definition of abbreviations: n/a = not available.

* Results are reported as fold change relative to control; $n = 4$ for each gene analyzed.

† All gene symbols are expressed as human homologs.

‡ Significantly different from control sample ($\alpha = 0.05$)

Discussion

Previously, we reported physical and chemical characterization of the BDS nanoparticles produced during incomplete combustion of the high volume petrochemical, 1,3-butadiene (**24,11**) and in addition, that human respiratory epithelial cells exhibited punctate cytoplasmic fluorescence following exposure to BDS (**11**). Here, we used fluorescence imaging techniques with organelle-specific probes, combined with analysis of gene expression to demonstrate that a) BDS-associated fluorescence localizes within lipid droplets and b) appearance of this fluorescence is correlated with enhanced expression of Phase I biotransformation and oxidative stress genes. The responses to BDS exposure are not limited to human respiratory epithelial cells, as mouse alveolar macrophages and adipocytes respond in a similar fashion.

The fluorescent responses begin with a diffuse cytoplasmic fluorescence that appears within the first 30 minutes after BDS exposure begins, progresses to fluorescence that localizes within lipid droplets over the next 2-4 hours, and is maintained over the next 72 hours. Lipid droplets were identified by co-localization of BDS fluorescence first with fluorescence of the cholesteryl-BODIPY probe and then with the fluorescent, lipid droplet-specific ADRP probe. The fluorescent responses are due to the PAHs, that are adsorbed to the surface of the BDS nanoparticles and which represent ~16% of the total weight of BDS (**11**). A concomitant time-dependent up-regulation of Ah receptor-associated Phase I biotransformation enzymes, including cytochrome P450s 1A1 and 1B1, revealed both by microarray and qRT-PCR analyses, is entirely consistent with the fluorescent responses. In addition, microarray data from BDS-exposed BEAS-2B cells reveal a time-dependent up-regulation of NRF2-mediated oxidative stress genes. We have reported similar patterns of gene up-regulation in lungs of mice that inhaled BDS daily for 4 days (**14**). The combined results indicate that exposure to BDS, and possibly to combustion products of other petrochemical volatiles, will result in increased cellular oxidative stress.

The localization of environmentally-derived PAHs within lipid droplets is noteworthy for at least two reasons. First, cigarette smoke and diesel exhaust, two ubiquitous sources of readily respirable, PAH-rich particles, would be expected to provide PAHs that could localize within lipid droplets of target cells. A number of the PAHs that are prominent in BDS also are prominent in cigarette smoke (**25**). Second, although it is reasonable to expect that inhaled hydrophobic compounds can be concentrated within lipid droplets of respiratory system cells, our results are the first of which we are aware, in which compounds other than those derived from lipid metabolism are localized within lipid droplets. The long-term availability of PAHs localized within lipid droplets in the lung or other tissues to PAH-metabolizing enzymes has not been investigated. There is a report that diesel exhaust particles on which B(a)P has been adsorbed can be recovered from the lungs of dogs 5 months after exposure (**26**). Similarly, we have found BDS particles in the lungs of mice twenty-eight days after a 2-day BDS exposure ended (unpublished observations). Thus, the combination of persistent lung irritation and the resulting inflammation from inhaled particles + delayed activation of PAH-metabolizing enzymes may promote a precancerous environment in the lung.

Acknowledgement: Figures 2A-C & 3A-C + Tables 2 & 3 originally appeared in:

Ref. **13**. Murphy G, Rouse R, Polk W, Henk W, Barker S, Boudreaux M, Floyd Z, Penn A. Combustion-derived hydrocarbons localize to respiratory cell lipid droplets and up-regulate biotransformation enzymes. *Am J Respir Cell Mol Biol* 2008;38 (5):532-540. The *Am J Respir Cell Mol Biol* is an official journal of the American Thoracic Society.

References

1. Bonvallot V, Baeza-Squiban A, Baulig A, Brulant S, Boland S, Muzeau F, Barouki R, Marano F. Organic compounds from diesel exhaust particles elicit a proinflammatory response in human airway epithelial cells and induce cytochrome p450 1A1 expression. *Am J Respir Cell Mol Biol* 2001;25:515-521.

2. Sayes CM, Reed KL, Warheit DB. Assessing toxicity of fine and nanoparticles: comparing in vitro measurements to in vivo pulmonary toxicity profiles. *Toxicol Sci* 2007;97:163-180.

3. Li N, Sioutas C, Cho A, Schmitz D, Misra C, Sempf J, Wang M, Oberley T, Froines J, Nel A. Ultrafine particulate pollutants induce oxidative stress and mitochondrial damage. *Environ Health Perspect* 2003;111:455-460.

4. Li N, Venkatesan MI, Miguel A, Kaplan R, Gujuluva C, Alam J, Nel A. Induction of heme oxygenase-1 expression in macrophages by diesel exhaust particle chemicals and quinones via the anti-oxidant responsive element. *J Immunol* 2000;165(6):3393-3401.

5. Murphy SA, BeruBe KA, Richards RJ. Bioreactivity of carbon black and diesel exhaust particles to primary clara and type ii epithelial cell cultures. *Occup Environ Med* 1999;56(12):813-819.

6. Ma JY, Ma JK. The dual effect of the particulate and organic components of diesel exhaust particles on the alteration of pulmonary immune/inflammatory responses and metabolic enzymes. *J Environ Sci Health C Environ Carcinog Ecotoxicol Rev* 2002;20(2):117-147.

7. Rao KM, Ma JY, Meighan T, Barger MW, Pack D, Vallyathan V. Time course of gene expression of inflammatory mediators in rat lung after diesel exhaust particle exposure. *Environ Health Perspect* 2005;113(5):612-617.

8. Saber AT, Jacobsen NR, Bornholdt J, Kjaer SL, Dybdahl M, Risom L, Loft S, Vogel U, Wallin, H.Cytokine expression in mice exposed to diesel exhaust particles by inhalation. Role of tumor necrosis factor. *Part Fibre Toxicol* 2006;3:4.

9. Li N, Alam J, Venkatesan MI, Eiguren-Fernandez A, Schmitz D, Di Stefano E, Slaughter N, Killeen E, Wang X, Huang A, Wang M, Miguel AH, Cho A, Sioutas C, Nel AE. Nrf2 is a key transcription factorthat regulates antioxidant defense in macrophages and epithelial cells: protecting against theproinflammatory and oxidizing effects of diesel exhaust chemicals. *J Immunol* 2004, 173: 3467-3481

10. International Agency for Research on Cancer. IARC Monographs on the Evaluation of Carcinogenic Risk to humans: Tobacco Smoking. IARC Monographs 1986;38:168-170.

11. Penn A, Murphy G, Barker S, Henk W, Penn L. Combustion-derived ultrafine particles transport organic toxicants to target respiratory cells. *Environ Health Perspect* 2005;113(8):956-963.

12. Catallo WJ, Kennedy CH, Henk W, Barker SA, Grace SC, Penn A. Combustion products of 1,3-butadiene are cytotoxic and genotoxic to human bronchial epithelial cells. *Environ Health Perspect* 2001;109(9):965-971.

13. Murphy G, Rouse R, Polk W, Henk W, Barker S, Boudreaux M, Floyd Z, Penn A. Combustion-derived hydrocarbons localize to respiratory cell lipid droplets and up-regulate biotransformation enzymes. *Am JRespir Cell Mol Biol* 2008;38 (5):532-540.

14. Rouse R, Murphy G, Boudreaux M, Paulsen D, Penn A. Soot nanoparticles promote biotransformation, oxidative stress, and inflammation in murine lungs. *Am J Respir Cell Mol Biol* 2008;39(2):198-207.

15. Pope CA, 3rd, Burnett RT, Thun MJ, Calle EE, Krewski D, Ito K, Thurston GD. Lung cancer, cardiopulmonary mortality, and long-term exposure to fine particulate air pollution. JAMA 2002; 287(9): 1131-1141.

16. Reddel RR, Ke Y, Gerwin BI, McMenamin MG, Lechner JF, Su RT, Brash DE, Park JB, Rhim JS, Harris CC. Transformation of human bronchial epithelial cells by infection with SV40 or adenovirus-12 SV40 hybrivirus, or transfection via strontium phosphate coprecipitation with a plasmid containing SV40 early region genes. *Cancer Res* 1988;48:1904-1909.

17. Mbawuike IN, Herscowitz HB. MH-S, a murine alveolar macrophage cell line: morphological, cytochemical and functional characteristics. *J Leukoc Biol* 1989;46:119-127.

18. Green H, Kehinde O. An established preadipose cell line and its differentiation in culture. II. Factors affecting the adipose conversion. *Cell* 1975;5:19-27.

19. Floyd ZE, Stephens JM. Interferon-gamma-mediated activation and ubiquitin-proteasome-dependent degradation of PPARgamma in adipocytes. *J Biol Chem* 2002;277:4062-4068.

20. Gould SJ, Keller GA, Hosken N, Wilkinson J, Subramani S. A conserved tripeptide sorts proteins to peroxisomes. *J Cell Biol* 1989;108:1657-1664.

21. Targett-Adams P, Chambers D, Gledhill S, Hope RG, Coy JF, Girod A, McLauchlan J. Live cell analysis and targeting of the lipid droplet-binding adipocyte differentiation-related protein. *J Biol Chem* 2003;278:15998-16007.

22. Fields WR, Desiderio JG, Putnam KP, Bombick DW, Doolittle DJ. Quantification of changes in c-myc mRNA levels in normal human bronchial epithelial (NHBE) and lung adenocarcinoma (A549) cells following chemical treatment. *Toxicol Sci* 2001;63:107-114.

23. Mamo S, Gal AB, Bodo S, Dinnyes A. Quantitative evaluation and selection of reference genes in mouse oocytes and embryos cultured in vivo and in vitro. *BMC Dev Biol* 2007;7:14.

24. Catallo WJ, Kennedy CH, Henk W, Barker SA, Grace SC, Penn A. Combustion products of 1,3-butadiene are cytotoxic and genotoxic to human bronchial epithelial cells. *Environ Health Perspect* 2001;109:965-971.

25. Grimmer G, Naujack KW, Dettbarn G. Gas chromatographic determination of polycyclic aromatic hydrocarbons, aza-arenes, aromatic amines in the particle and vapor phase of mainstream and sidestream smoke of cigarettes. *Toxicol Lett* 1987;35:117-124.

26. Gerde P, Muggenburg BA, Lundborg M, Dahl AR. The rapid alveolar absorption of diesel soot-adsorbed benzo[a]pyrene: bioavailability, metabolism and dosimetry of an inhaled particle-borne carcinogen. *Carcinogenesis* 2001;22:741-749.